Am J Transl Res 2018;10(5):1295-1309
www.ajtr.org /ISSN:1943-8141/AJTR0073113

Original Article

Exogenous glutathione contributes to cisplatin resistance in lung cancer A549 cells

Dong Lan[1#], Li Wang[2#], Rongquan He[1], Jie Ma[1], Yehong Bin[1], Xiaojv Chi[1], Gang Chen[3*], Zhengwen Cai[2*]

Departments of [1]Medical Oncology, [2]Pathology, First Affiliated Hospital of Guangxi Medical University, No. 6 Shuangyong Road, Nanning 530021, Guangxi Zhuang Autonomous Region, P. R. China; [3]Department of Medical Oncology, Second Affiliated Hospital of Guangxi Medical University, No. 166 Daxuedong Road, Nanning 530007, Guangxi Zhuang Autonomous Region, P. R. China. [#]Equal contributors and co-first authors. [*]Equal contributors.

Received January 20, 2018; Accepted April 26, 2018; Epub May 15, 2018; Published May 30, 2018

Abstract: Background: Recent studies have reported that an elevated intracellular glutathione (GSH) level is associated with resistance of non-small cell lung cancer (NSCLC) cell lines to cisplatin (CDDP). It is well-known that GSH is widely used in the clinic as a hepatoprotective agent. However, whether exogenous GSH can affect the sensitivity of NSCLC cells to CDDP remains unclear. The aim of this study is to evaluate the role of exogenous GSH in the resistance of A549 cells to CDDP. Methods: The effect of GSH and CDDP on the proliferation of A549 cells was analyzed by MTT assay. Subsequent experiments were conducted in A549 cells divided into four groups: control group (untreated cells), GSH group (treated with 120 μg/ml GSH for 48 h), CDDP group (treated with 10 μg/ml CDDP for 48 h) and CDDP+GSH group (treated with 10 μg/ml CDDP+120 μg/ml GSH for 48 h). Apoptosis was detected by flow cytometry. Light microscopy, fluorescence microscopy and electron microscopy were performed to study morphologic and ultrastructural differences among the four groups of cells. Intracellular GSH level and γ-GCS expression were determined by immunohistochemistry (IHC). Cellular platinum uptake was assessed by inductively coupled plasma mass spectrometry (ICP-MS). Quantitative RT-PCR analysis was performed to measure the expression of caspase3, caspase9, bax, bcl-2 and MDR-1. Western blot analysis was conducted to examine the protein levels of GST-π, MRP-1 and P-gp. Results: Growth inhibition and apoptosis were reduced in A549 cells in the CDDP+GSH group compared to those in the CDDP group 48 h post-treatment. Alterations in cellular morphology and ultrastructure, as well as typical characteristics of apoptosis, were observed. Intracellular GSH and γ-GCS levels were elevated by exogenous administration of GSH; in contrast, cellular platinum concentration fell rapidly. Relative to the CDDP group, the CDDP+GSH group exhibited 47.92%, 47.82% and 63.75% downregulation in caspase3, caspase9 and bax mRNA expression, respectively, and a 2.17-fold increase in bcl-2 mRNA level. In addition, there were 1.58-fold and 2.67-fold increases in the level of GST-π and MRP-1, respectively; however, the changes in MDR-1 and P-gp levels were not statistically significant. Conclusions: Our data demonstrated that exogenous GSH used as hepatinica in the clinic could induce resistance of A549 cells to CDDP by inhibiting apoptosis, elevating cellular GSH levels, inactivating the mitochondria-mediated signaling pathway, and increasing the expression of GST-π, γ-GCS and MRP1 to increase CDDP efflux.

Keywords: A549 cells, GSH, CDDP, apoptosis, platinum concentration

Introduction

Lung cancer is the leading cause of cancer-related death in humans worldwide, accounting for 1.3 million deaths annually [1]. Despite considerable progress over the past few decades in the systemic treatment of lung cancer, there has been little improvement in patient outcomes, as many patients ultimately relapse and their tumors become resistant to initial therapy [2]. Non-small cell lung cancer (NSCLC) accounts for 85% of all lung cancer cases and is commonly insensitive and intrinsically resistant to original chemotherapy. Cisplatin (CDDP)-based chemotherapy regimens have been the standard therapeutic strategy in advanced stage NSCLC. However, published data reveal the incidence of resistance to CDDP in up to 63% of NSCLC [3]. Resistance remains an obstacle in chemotherapy and seriously influences the survival rate of NSCLC patients.

Glutathione (GSH) is an important cellular antioxidant and detoxification system in the body,

composed of glutamate, cysteine and glycine. GSH plays a critical role in suppressing oxidative stress, protecting cells from free radical damage, and detoxifying chemotherapeutic compounds. In addition, GSH is important for regulating proliferation and death of cells. As a result, disturbances in GSH homeostasis have been implicated in the occurrence and progression of various human diseases, including cancer. In many tumors, such as lung cancer, the GSH system is often dysregulated, resulting in drug resistance [4]. Several studies have shown that the expression of glutathione-S-transferase (GST) family members, antioxidants such as GSH, drug efflux proteins known as multidrug resistance protein (MRP) family and P-glycoprotein (P-gp) is increased in NSCLC [5-7]. The phenomenon of drug resistance in NSCLC is commonly associated with GST-mediated GSH conjugation of various anticancer agents leading to the formation of less toxic GSH-drug complexes called GS-X that are less active and more water soluble and can be readily exported from the cells via MRPs encoded by ABCC1, ABCC2 and ABCB1 (also known as MDR-1) [8]. Previous studies have reported that exposure of cultured cells to CDDP leads to the development of CDDP resistance, which is correlated with increased cellular GSH levels [9-11]. Moreover, GSH depletion by buthionine-sulfoximine (BSO), a selective inhibitor of γ-Glutamylcysteine synthetase (γ-GCS), has been associated with increased sensitivity to CDDP [12-14].

These studies have widely demonstrated that intracellular GSH levels play an important role in resistance to CDDP [15-17]. However, apart from these results, the relationship between external GSH and CDDP resistance has not been reported. Chen et al. demonstrated that pretreatment of A549 cells with 100 μM GSH markedly attenuated denbinobin-induced apoptosis in A549 cells by 77.0±4.1% [18]. Consequently, we speculated that exogenous GSH can induce resistance of NSCLC cells to CDDP. However, GSH is regarded as a hepatoprotective agent and is widely used in the clinic. Therefore, it is important to confirm the validity of our hypothesis. If our hypothesis is confirmed, clinical use of GSH needs to be reconsidered.

To further explore whether GSH can affect the sensitivity of NSCLC cells to CDDP, A549 cells (a human pulmonary adenocarcinoma cell line) were treated with CDDP and GSH; then, the apoptosis rate, intracellular GSH level, cellular platinum concentration, apoptosis-related genes and GSH-related enzyme systems were analyzed.

Materials and methods

Materials

GSH was obtained from LvYe Pharmaceutical Co., Ltd, China. CDDP, penicillin and streptomycin were obtained from QiLu Pharmaceutical Co., Ltd, China. Ham's F-12 medium and fetal bovine serum (FBS) were purchased from HyClone, USA. 3-(4,5-dimethylthiazol-2-yl-2,5-diphenyl tetrazolium bromide (MTT), dimethyl sulfoxide (DMSO) and phosphate-buffered saline (PBS) were purchased from Sigma-Aldrich (St. Louis, MO, USA). Propidium iodide (PI) and Annexin-V-FITC (AV) were purchased by from KeyGEN Biotech., China. Antibodies against GSH, γ-GCS and β-actin were purchased from Boster, China. Antibodies against GST-π, P-gp and MRP-1 were purchased from Abcam, USA. All other chemicals and reagents were purchased from Sigma, USA and used as indicated.

Cell culture

The human pulmonary type II epithelial adenocarcinoma cell line A549 was obtained from Shanghai Institute of Cell Biology in China and cultured in Ham's F-12 medium with 10% FBS and antibiotics (100 U/ml penicillin and 100 μg/ml streptomycin). The cells were cultured at 37°C in a humidified atmosphere containing 5% CO_2.

Cell proliferation assay

Cells were seeded in 96-well microplates at a density of 5.0×10^3 cells per well. First, the cells were cultured with CDDP alone at 2.5, 5, 10, 20 and 40 μg/ml for 48 h. For the GSH-treated groups, the cells were treated for 48 h with the following concentrations of GSH: 60, 120, 240, 480, 960 μg/ml. MTT assay (the details are included below) was used to detect the proliferation of A549 cells after treatment with CDDP or GSH. From the above experiments, the 10 μg/ml concentration of CDDP was determined for use in the following experiments. Next, A549 cells were co-incubated with 10 μg/ml of

CDDP and an increasing concentration of GSH (range from 60 μg/ml to 960 μg/ml) for 48 h. Then, the cells in each well were exposed to 10 μl MTT (5.0 mg/ml) for another 4 h at 37°C. Finally, the supernatant was removed and 150 μl DMSO was added to determine the OD at 570 nm using an enzyme-linked immunosorbent assay reader (Thermo, USA). The proliferation rate was calculated by using the following equation: growth inhibition rate= [1-(OD sample-OD blank)/(OD control-OD blank)]×100%; cell viability rate= (OD sample-OD blank)/(OD control-OD blank)×100%. The viability of the untreated cells was considered to be 100%. Five wells were used for each group, and the experiment was repeated three times.

Experimental groups

The cells were divided into four groups for the subsequent experiments: control group (untreated A549 cells), GSH group (A549 cells were cultured with 120 μg/ml GSH for 48 h), CDDP group (A549 cells were exposed to 10 μg/ml CDDP for 48 h), CDDP+GSH group (A549 cells were cultured in 10 μg/ml CDDP+120 μg/ml GSH for 48 h).

Flow cytometric (FCM) analysis

A549 cells were inoculated in 6-well plates at 1.0×10^6 cells/well. After the various treatments for 48 h, the cells were collected and digested with 0.25% trypsin at 37°C for 3-4 min. The cells were gently pipetted and collected by centrifugation at 1000 rpm for 5 min; next, the cells were washed twice with cold PBS and resuspended in PBS. Then, the cells were stained with AV and PI at 0°C according to the manufacturer's instruction. Apoptosis was analyzed with a flow cytometer (BD Biosciences, USA). The percentage of apoptotic cells was determined by FCM analysis. Phosphatidylserine (PS) was used as a surface marker of early apoptotic cells and detected by AV (a recombinant PS-binding protein with a high affinity for externalized PS). PI was used to examine late apoptosis and necrosis. The cells were distinguished into four categories by flow cytometry, namely, viable (AV- and PI-negative), early apoptotic (AV-positive and PI-negative), late apoptotic (AV- and PI-positive) and necrotic (AV-negative and PI-positive) cells.

Cell morphological observation with light microscope, fluorescence microscope and transmission electron microscope (TEM)

A549 cells were seeded in six-well plates at 1.0×10^6 cells/ml and divided into four groups. First, A549 cells in each group were observed under a light microscope (BX40, Olympus, Japan). Then, morphological changes were further analyzed using acridine orange/propidium iodide (AO/PI) double staining assay. After 48 h, untreated and treated A549 cells were collected and washed twice with PBS. Then, the cells were stained with 10 μg/mL of AO/PI. The stained cells were then examined under a fluorescence microscope (BX53, Olympus, Japan) within 30 min. Furthermore, we observed microstructural changes in A549 cells with a TEM (JEOL JEM-2100, Japan). Cells in each group were digested, collected and resuspended at a density of 1.0×10^6 cells/ml. The samples were centrifuged at 1000 rpm for 10 min, and the supernatant was discarded. The A549 cells were fixed with 3% glutaraldehyde in 0.1 M cacodylate buffer (pH 7.3) at 4°C for 4 h. The samples were post-fixed with 2% osmium tetraoxide at 4°C for 2 h, dehydrated, and embedded in epoxy resin. Ultrathin sections (80 nm) were then stained with uranyl acetate and lead citrate. The samples were observed with the TEM under a 200 kV electron acceleration voltage.

Analysis if intracellular GSH level by immunohistochemistry (IHC)

A549 cells were divided into four groups and seeded on glass slides placed in six-well plates. After 48 h of treatment, the slides were washed with PBS and air dried at room temperature. The cells were fixed in 4% paraformaldehyde, permeabilized for 1 h at room temperature and then incubated with primary antibodies including rabbit anti-GSH (1:200 dilution) and rabbit anti-γ-GCS (1:200 dilution) overnight at 4°C. Subsequently, examination was performed using the ABC Elite Kit (Boster, China) with biotinylated goat anti-rabbit secondary antibody at room temperature for 1 h. The slides were developed with DAB, counterstained with a nuclear dye and then detected under a microscope (BX40, Olympus, Japan). The results were calculated as percentage of the mean value. The percentage of cells that stained positive was assigned to one of the following

grades: (0) <5%; (1) 5-25%; (2) 25-50%; (3) 50-75%; and (4) >75%. The staining intensity was independently graded on the following scale: (0) none; (1) weak; (2) moderate; (3) strong; and (4) intense.

Quantification of intracellular platinum concentration by inductively coupled plasma mass spectrometry (ICP-MS)

To detect intracellular platinum concentration, 1.0×10^6 A549 cells from each treatment group were collected from six-well plates. The cells were washed three times in cold PBS, digested, harvested and centrifuged at 3000 rpm for 30 min. The cells were suspended with 1 ml PBS, and then 5 ml 1% nitric acid (HNO3) was added to lyse the cells at 37°C for 20 min. The lysates were diluted to 25 ml with distilled water. Intracellular platinum (Pt) concentrations were determined by ICP-MS (Agilent 7500ce, Germany). Platinum concentrations were expressed as ng/ml.

RNA preparation and RT-PCR

To determine mRNA levels of caspase3, caspase9, bax, bcl-2 and MDR-1, A549 cells were cultured under the four different conditions mentioned above. After treatment for 48 h, total RNA was extracted using TRIzol reagent (Invitrogen, USA) according to the manufacturer's instructions. Reverse-transcribed complementary DNA was synthesized with the RevertAid First Strand cDNA Synthesis Kit (Fermentas, USA). RT-PCR was performed with Maxima SYBR Green/ROX qPCR Master Mix (Fermentas, USA) using the CFX96 Real-Time PCR Detection System (Bio-Rad, USA). The sequences of primers used in the experiment are as follows: caspase3 (348 bp), forward 5'-TTGTGGAATTGATGCGTGAT GT-3' and reverse 5'-CATCCTTTGAATTTCGCAAGA-3'; caspase9 (264 bp), forward 5'-TGTGAACTTCTGCCGTGAGTC-3' and reverse 5'-CATCCATCTGTGCCGTAGACA-3'; bax (178 bp), forward 5'-AAGCTGATCGAGTGTCTCAAG-3' and reverse 5'-CAAAGTAGAAAAGGGCGACAAC-3'; bcl-2 (135 bp), forward 5'-ACATCCTATCAA CAACAA-3' and reverse 5'-GTATCTACACTACAGTCTTA-3'; and MDR-1 (183 bp), forward 5'-CAGTCAAGTTCAGAGTCTTCAGA-3' and reverse 5'-GGCAGTCAGTTACAGTCCAA-3'. Transcript levels were normalized to the level of β-actin (153 bp) with the following primers: forward 5'-ACACTGTGCCCATCTACG-3' and reverse 5'-TGTCACGCACGATTTCC-3'. The fold changes were calculated by the delta-delta Ct method. All experiments were performed in triplicate.

Western blot analysis

To determine the protein levels of GST-π, P-gp and MRP1, total protein was collected from the four groups of cells. The cells were washed twice with cold PBS and lysed in ice-cold Radio Immunoprecipitation Assay (RIPA) buffer (Boster, China). The lysed samples were incubated with protease inhibitor (Sigma, USA) for 30 min in an ice bath and then centrifuged at 12,000 rpm for 5 min at 4°C. Equal amounts of extracts (80 μg protein) were subjected to 10% sodium dodecyl sulfate-polyacrylamide gel electrophoresis (SDS-PAGE) and transferred onto a nitrocellulose membrane. After being treated in Tris-buffered saline with 0.05% Tween 20 (TBS-T) and 5% dry powdered milk for 2 h at room temperature, the membrane was washed three times with TBS-T for 5 min each time. Next, the membrane was incubated overnight at 4°C with primary antibodies against GST-π, P-gp, MRP1 and β-actin, washed with TBS-T, incubated with the corresponding horseradish peroxidase (HRP)-conjugated secondary antibodies (Boster, China) for 2 h at room temperature and then washed again with TBS-T. Finally, protein expression was detected with the ECL plus chemiluminescence detection kit (Beyotime Biotech, China). The films were scanned, and quantitation was performed with Optiquant software (GBOX/CHEM, USA). Protein levels were normalized by that of β-actin. The experiment was repeated three times.

Statistical analysis

MTT assay, FCM analysis, IHC, ICP-MS, RT-PCR and WB were repeated at least three times. The data are graphically represented as the mean ± standard error of the mean (mean ± SD). Statistical comparison between groups was conducted by analysis of variance (ANOVA) using SPSS (version 17.0). When the means of two datasets were compared, significance was determined by two-tailed Student's t-test. Differences were considered significant when $P<0.05$.

Results

Effect of GSH and CDDP on proliferation of A549 cells detected by MTT

Cells were separately treated with the indicated concentrations of CDDP and GSH, and MTT

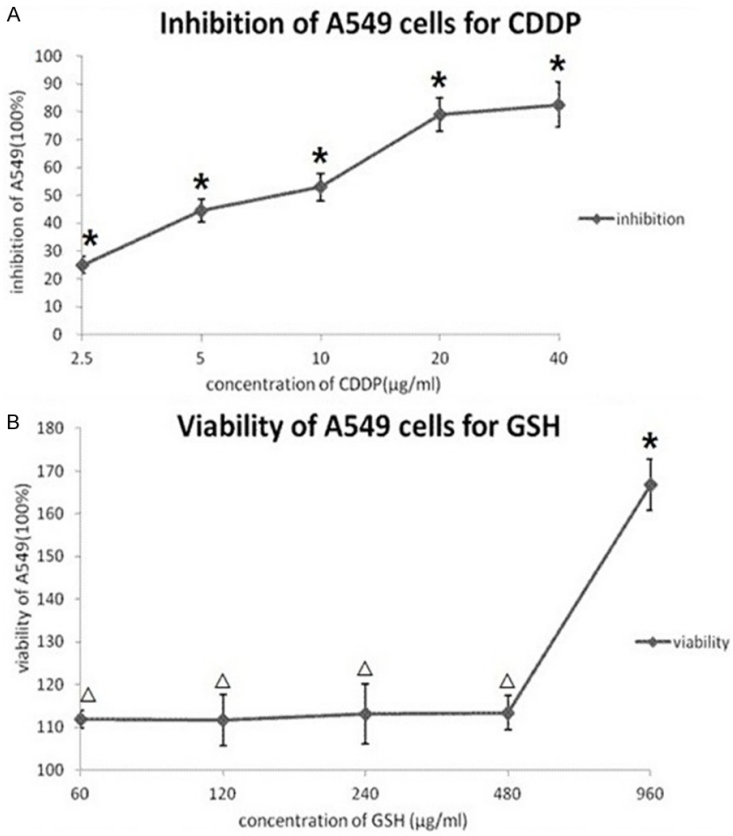

Figure 1. Effect of CDDP and GSH on A549 cell individually. A. A549 cells were treated with increasing concentrations of CDDP for 48 h. B. A549 cells were treated with various concentrations of GSH for 48 h. Cell viability was detected using MTT assay. Each point represents the mean ± SD from three measurements, and *presents significantly difference (P<0.01), Δpresents no statistical significance (P>0.05).

Table 1. Effect of CDDP and GSH on A549 cells (x±s, n=3)

Group	Inhibition rate (100%)	*P*-value
Control group	Not applicable	Not applicable
10 μg/ml CDDP	52.93±3.96	0.00*
10 μg/ml CDDP+60 μg/ml GSH	41.68±3.98	0.00#
10 μg/ml CDDP+120 μg/ml GSH	28.03±4.05	0.00#
10 μg/ml CDDP+240 μg/ml GSH	21.58±3.77	0.00#
10 μg/ml CDDP+480 μg/ml GSH	15.00±3.45	0.00#
10 μg/ml CDDP+960 μg/ml GSH	7.00±2.01	0.00#

The data represent the mean of five independent replicates, combined to generate the mean ± SD for each concentration. *P<0.01 compared to the control group; #P<0.01 compared to the 10 μg/ml CDDP group.

assay was used to measure the viability of cells. The IC_{50} value of CDDP in A549 cells calculated by SPSS 17.0 was 7.40±0.32 μg/ml. Therefore, we chose the 10 μg/ml concentration of CDDP, which was close to the IC_{50} value for the subsequent experiments. We demonstrated that increasing concentrations of CDDP inhibited the proliferation of A549 cells in a dose-dependent manner (**Figure 1A**), and the inhibition was statistically significant compared to the untreated cells and among cells treated with various concentrations of CDDP (P<0.05). Within a certain concentration range (60-480 μg/ml), GSH promoted the proliferation of A549 cells only by approximately 10% relative to untreated cells, and the difference was significant (P<0.05). Moreover, the difference in cell proliferation in response to 60 to 480 μg/ml of GSH was very small (**Figure 1B**) and was not statistically significant (P>0.05). However, 960 μg/ml GSH markedly induced proliferation of A549 cells relative to the untreated cells, and the difference was significant (P<0.05).

The results of MTT assay with 10 μg/ml CDDP and various doses of GSH indicated that GSH led to a significant suppression in the inhibition of A549 cells in response to CDDP in a dose-dependent manner (**Table 1**). GSH at 60, 120, 240, 480 and 960 μg/ml concentrations markedly attenuated CDDP-induced apoptosis in A549 cells by 10.66±4.36%, 24.34±3.33%, 30.66±4.36%, 37.32±3.23% and 45.00±2.08%, respectively. As shown in **Table 1**, the inhibition of A549 cells cultured with CDDP and GSH was significantly lower than that of the cells treated with CDDP alone (P<0.05). These data clearly show that GSH might effectively induce CDDP-resistance in A549 cells.

Detection of apoptosis using FCM analysis

To evaluate whether A549 cells undergo apoptosis and to investigate the biochemical characteristics of apoptosis, cells in the four groups

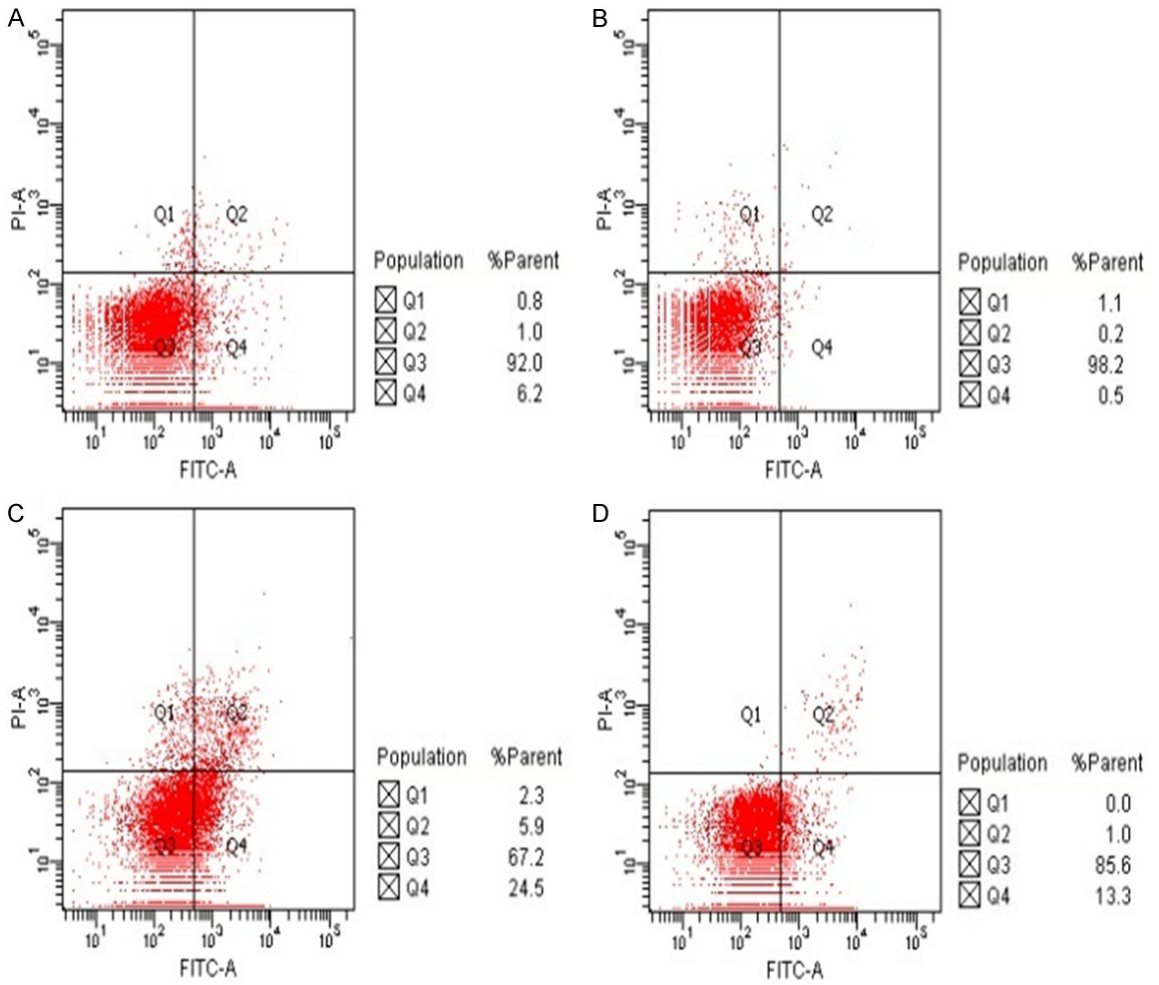

Figure 2. Apoptosis of A549 cells detected by FCM. A. Untreated A 549 cells. B. A549 cells treated with 120 μg/ml GSH for 48 h. C. A549 cells treated with 10 μg/ml CDDP for 48 h. D. A549 cells treated with 10 μg/ml CDDP+120 μg/ml GSH for 48 h. Q3 quadrant indicates viable cells (AV-/PI-). Q4 quadrant indicates early apoptotic cells (AV+/PI-). Q2 quadrant indicates late apoptotic cells (AV+/PI+) and Q1 quadrant indicates necrotic cells (AV-/PI+).

were stained with AV and PI for flow cytometric analysis. As illustrated in **Figure 2**, quadrants Q2 and Q4 represent total apoptotic cells. Apoptosis rates in the four groups were as follows: control group 6.5±0.7%, GSH group 1.0±0.3%, CDDP group 35.1±4.6%, CDDP+GSH group 16.7±2.2%. GSH treatment at 120 μg/ml for 48 h increased the viability of cells and reduced the proportion of early apoptotic cells compared to that in the untreated cells, and the difference was significant ($P<0.05$); 10 μg/ml CDDP induced pronounced apoptosis in A549 cells relative to the untreated cells, and the difference was significant ($P<0.05$); Compared to that in the CDDP group, the overall rate of apoptosis decreased notably in the CDDP+GSH group ($P<0.05$). These outcomes were consistent with the results of the MTT assay. The data described above illustrated that extrinsic GSH induced resistance of A549 cells to CDDP by inhibiting cell apoptosis.

Detection of effects of CDDP and GSH on cell morphology by light microscopy, fluorescence microscopy and transmission electron microscopy

The typical morphological features of apoptosis are cell shrinkage, nuclear pyknosis and formation of apoptotic bodies. The increase in cytoplasmic density and condensation of organelles result in cell shrinkage, and chromatin condensation is the most noticeable characteristic of early apoptosis [19]. Blebbing of plasma membrane with tightly packed organelles is a distinct feature of late apoptosis [20].

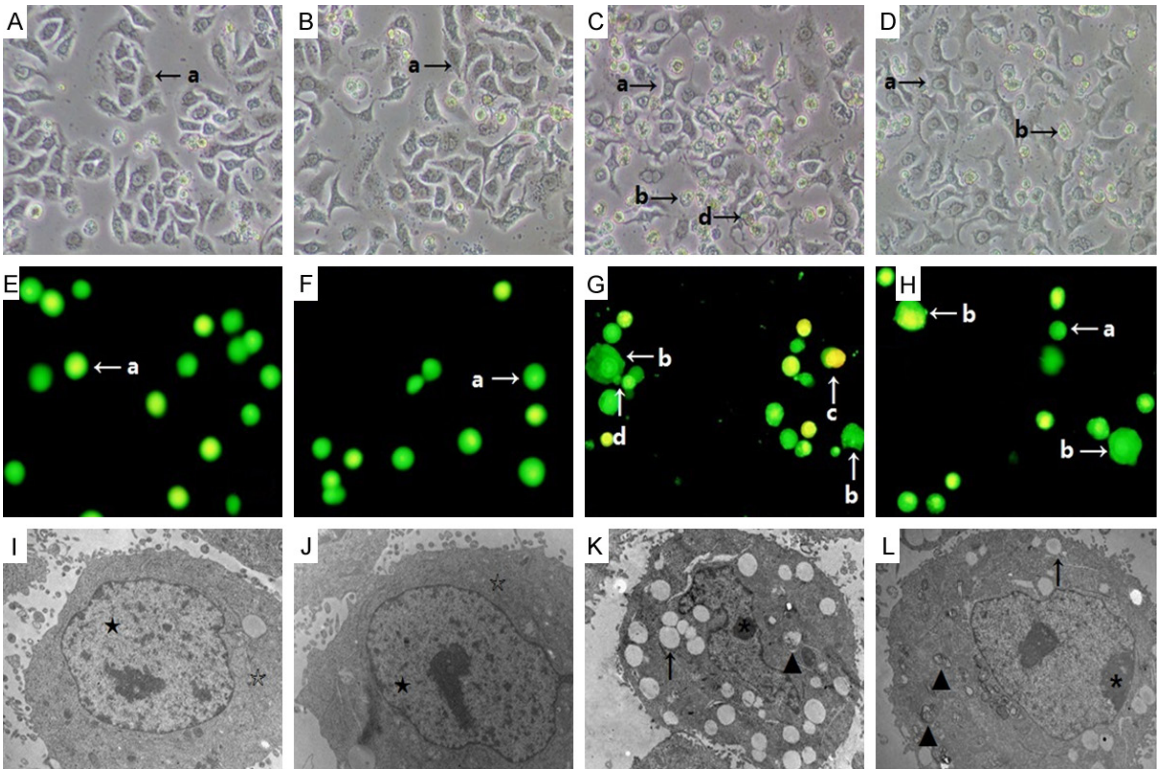

Figure 3. Morphology changes of A549 cells exmined by light microscope, fluorescence microscope and TEM. A, E, I: Untreated A549 cells. B, F, J. A549 cells treated with 120 μg/ml GSH for 48 h. C, G, K. A549 cells treated with 10 μg/ml CDDP for 48 h. D, H, L. A549 cells treated with 10 μg/ml CDDP+120 μg/ml GSH for 48 h. A-D. Images under light microscope (200×). E-H. Images under fluorescence microscope (200×). Marked a: Viable cells. Marked b: Apoptotic cells. Marked c: Late apoptotic cells. Marked d: Apoptotic body. I-L. Images of TEM (500×). ★: The nuclear chromatin was homogeneous. ☆: The intracytoplasmic rough endoplasmic reticulum was dense. *: The nuclear chromatin coagulated and gathered in the vicinity of the nuclear membrane. ▲: The cytoplasmic mitochondria were swollen. ↑: The endoplasmic reticulum expanded.

Morphological changes in the four groups were observed after 48 h of treatment by light microscopy, fluorescence microscopy and transmission electron microscopy. The untreated cells were short, spindle-shaped or triangular and exhibited characteristics similar to that of adherent epithelial cells by microscopy (**Figure 3A**). It is noteworthy that after 48 h, the untreated cells remained intact and displayed normal structures, with intact, green-colored nuclear structures as detected by fluorescence microscopy (**Figure 3E**). The chromatin of the untreated cells was homogeneous, and the cells displayed dense intracytoplasmic rough endoplasmic reticulum, abundant ribosomes and numerous healthy microvilli on the surface by transmission electron microscopy (**Figure 3I**). There were no obvious morphological changes in cells incubated with 120 μg/ml GSH for 48 h compared with the untreated cells (**Figure 3B**, **3F**, **3J**). In the CDDP group, the cells became smaller in size and rounded, and some cells sloughed off; furthermore, chromatin condensation and presence of cytoplasmic vacuoles and apoptotic bodies were frequently observed by microscopy (**Figure 3C**). The early apoptotic cells were detected via the binding of AO with the fragmented DNA giving rise to bright green fluorescence; the late apoptotic cells were detected by the presence of a reddish-orange color by fluorescence microscopy because of the binding of PI to denatured DNA (**Figure 3G**). With TEM, it was observed that the chromatin coagulated and gathered near the nuclear membrane, the endoplasmic reticulum expanded, and the mitochondria were swollen. The number of microvilli on the cell surface decreased (**Figure 3K**). Compare to that in the CDDP group, the number of pyknotic, blebbing and shedding cells was lower in the CDDP+GSH group (**Figure 3D**), and the extent of chromatin condensation and apoptotic bodies was reduced (**Figure 3H**); furthermore, chromatin condensation and mitochondrial swelling were

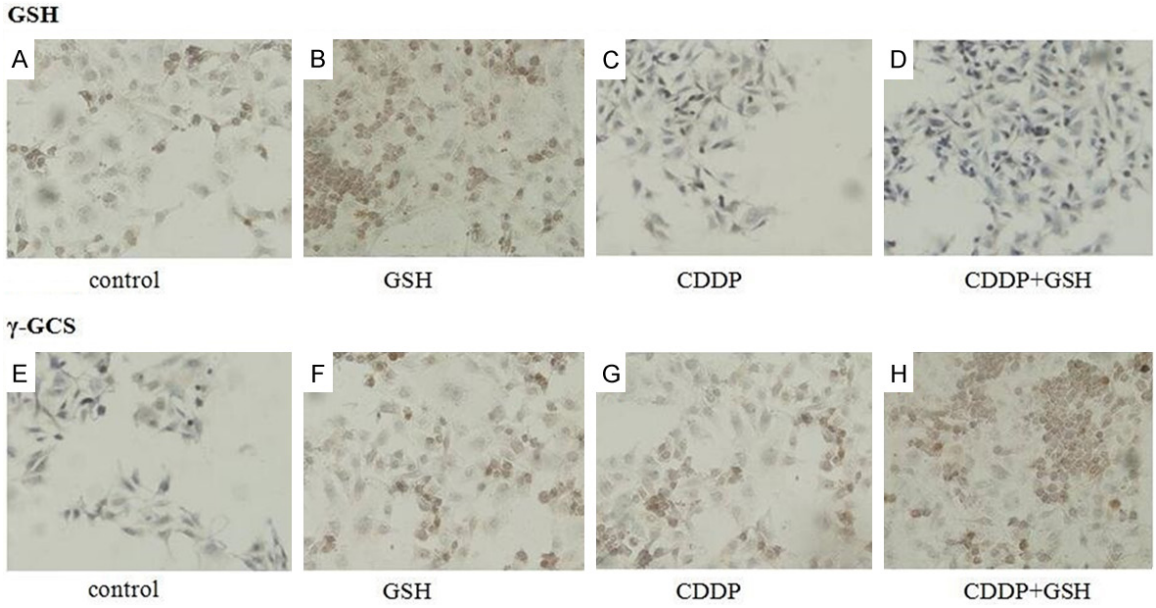

Figure 4. IHC analysis of GSH and γ-GCS expression in the control group, GSH group, CDDP group and CDDP+GSH group. A, E: Untreated A549 cells. B, F: A549 cells treated with 120 μg/ml GSH for 48 h. C, G: A549 cells treated with 10 μg/ml CDDP for 48 h. D, H: A549 cells treated with 10 μg/ml CDDP+120 μg/ml GSH for 48 h. A-D: IHC analysis of GSH expression. E-H: IHC analysis of γ-GCS expression.

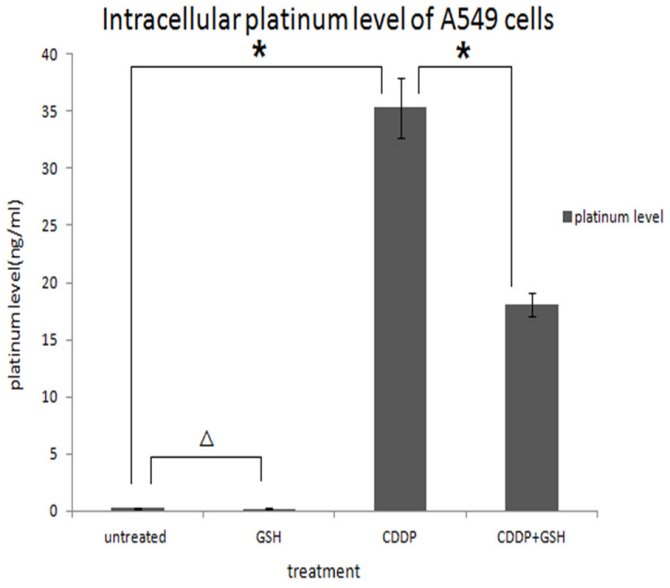

Figure 5. Quantification of intracellular platinum level by ICP-MS. Intracellular platinum level was determined by ICP-MS analysis with exponentially growing cells undergone different treatment for 48 h. Date are expressed as mean ± SD from three independent experiments (n=3) (ΔP>0.05, *P<0.01).

Immunohistochemistry

To measure intracellular GSH and γ-GCS protein expression in the four groups of A549 cells, the IHC staining method was employed. As illustrated in **Figure 4**, both GSH and γ-GCS were found to be localized in the cytoplasm. The expression of GSH protein in the control group was weaker than that of the GSH group but stronger than that of the CDDP group. Moreover, GSH level was higher in the CDDP+GSH group relative to that in the CDDP group. On the other hand, GSH treatment and CDDP treatment led to a marked increase in γ-GCS protein expression compared to control treatment. Interestingly, γ-GCS expression in the CDDP+GSH group was much higher compare to that of the CDDP group or GSH group.

Cellular uptake of platinum is reduced by GSH

To determine platinum accumulation in A549 cells in the four groups, intracellular platinum levels were quantified by ICP-MS (**Figure 5**). Across the four groups, findings from ICP-MS analysis demonstrated that there was no obvious difference in intracellular platinum levels

relieved, and the number of microvilli was increased (**Figure 3L**). These results thus revealed the presence of typical morphological features of apoptosis in CDDP-treated A549 cells; more importantly, GSH reduced the dama-ge induced by CDDP on A549 cells.

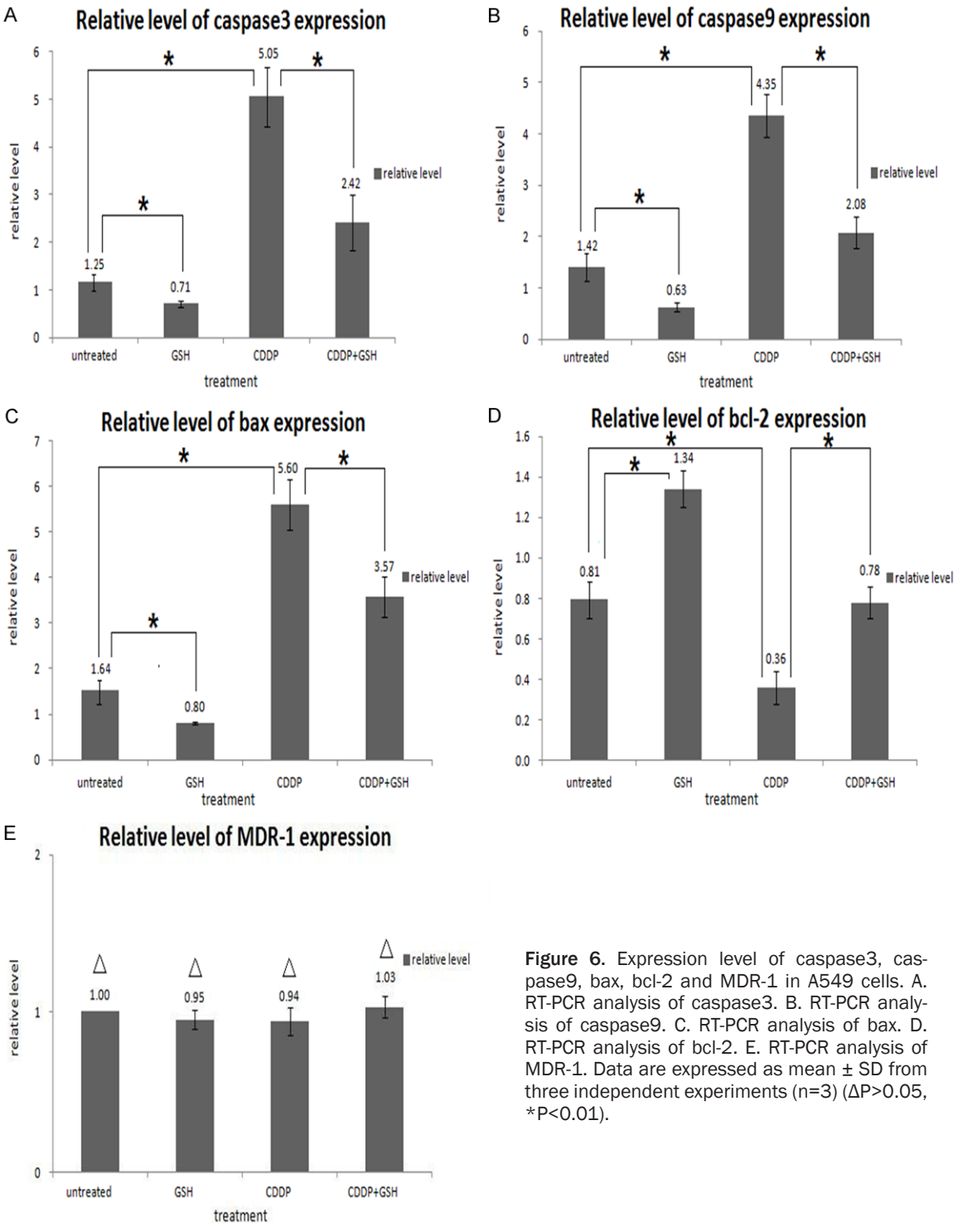

Figure 6. Expression level of caspase3, caspase9, bax, bcl-2 and MDR-1 in A549 cells. A. RT-PCR analysis of caspase3. B. RT-PCR analysis of caspase9. C. RT-PCR analysis of bax. D. RT-PCR analysis of bcl-2. E. RT-PCR analysis of MDR-1. Data are expressed as mean ± SD from three independent experiments (n=3) (ΔP>0.05, *P<0.01).

between the cells treated with 120 μg/ml GSH for 48 h and the untreated cells (0.22±0.03 ng/ml vs. 0.25±0.04 ng/ml, t=-0.85, P>0.05). Furthermore, treatment with 10 μg/ml CDDP for 48 h significantly increased the uptake of platinum relative to the untreated cells (35.33±2.64 ng/ml vs. 0.25±0.04 ng/ml, t=23.02, P<0.05). However, exposure to CDDP and GSH markedly reduced the uptake of platinum compared to CDDP alone (18.11±1.05 ng/ml vs. 35.33±2.64 ng/ml, t=10.50, P<0.05). These results supported the conclusion that

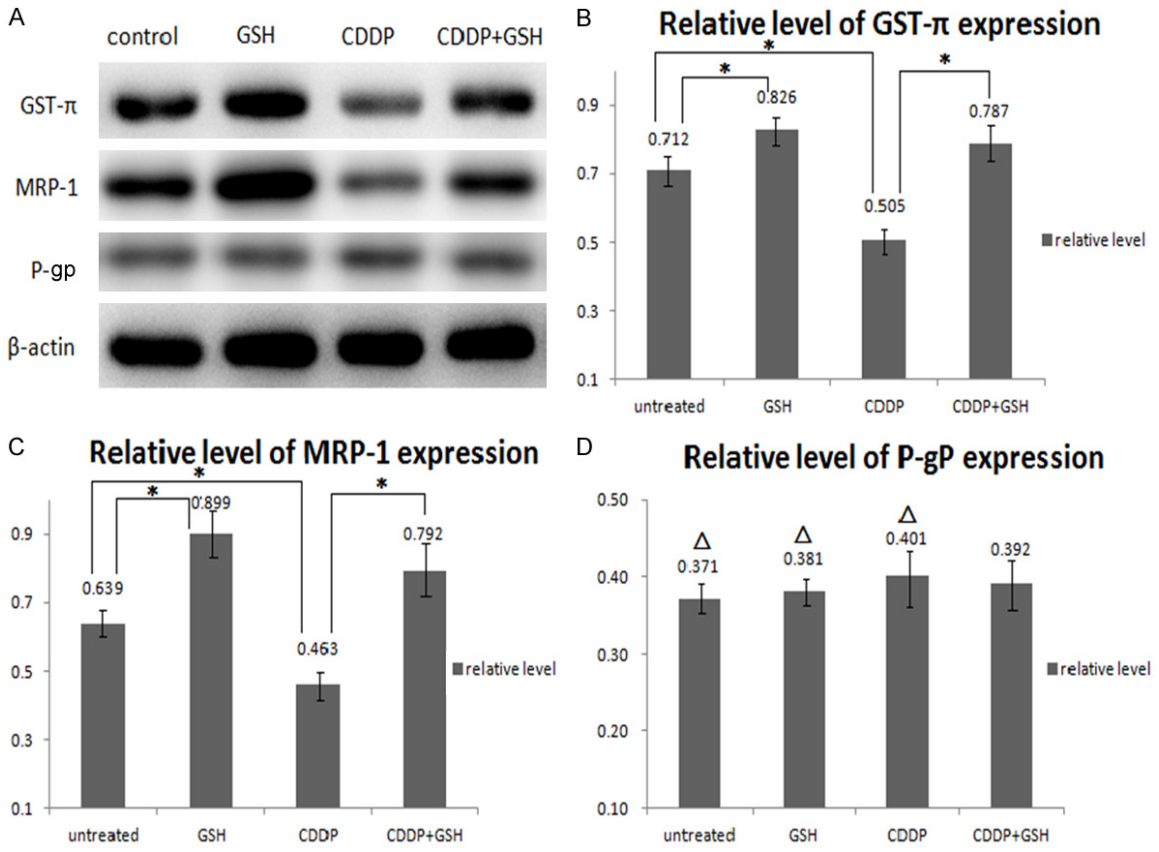

Figure 7. Protein levels of GST-π, MRP-1 and P-gp in A549 cells analyzed by Western blotting. A. Protein levels of GST-π, MRP-1 and P-gp. β-actin was used as an internal control. B. Analysis of GST-π protein expression. C. Analysis of MRP-1 protein expression. D. Analysis of P-gp protein expression. All experiments were performed in triplicate. The data are expressed as the mean ± SD from three independent experiments (n=3) (ΔP>0.05, *P<0.01).

treatment with GSH, i.e., exogenous GSH, has the potential to deplete intracellular platinum in A549 cells.

Gene expression validation by RT-PCR

To determine the expression of caspase3, caspase9, bax, bcl-2 and MDR-1 in A549 cells, quantitative RT-PCR was performed in the treated and untreated cells. As shown in **Figure 6**, RT-PCR showed the relative gene expression levels from each group of A549 cells. Apoptosis-related genes such as caspase3, caspase9 and bax were significantly downregulated in the cells treated with 120 μg/ml GSH compared to the corresponding levels in the untreated cells ($P<0.05$), but bcl-2 was significantly upregulated in the GSH group compared to that in the control group ($P<0.05$). Conversely, exposure to 10 μg/ml CDDP induced upregulation of caspase3, caspase9, and bax and downregulation of bcl-2 compared to the control treatment ($P<0.05$). Furthermore, in contrast to the CDDP group, the CDDP+GSH group exhibited reduced expression of caspase3, caspase9, bax and enhanced expression of bcl-2 ($P<0.05$). Interestingly, the RT-PCR results showed that the mRNA expression of MDR-1 in the untreated A549 cells was very low, and the difference in MDR-1 levels among the control, GSH, CDDP and CDDP+GSH groups were not significant ($P>0.05$).

Protein expression determined by WB

WB analysis was used to determine the protein level of GST-π, MRP-1 and P-gp as shown in **Figure 7**. β-actin was used as an internal control. Protein expression in each group of A549 cells was quantified in the following bar graphs. In this study, we established that exogenous GSH increased the expression of MPR1 and GST-π relative to control ($P<0.05$), but treatment with CDDP clearly downregulated the

level of MPR1 and GST-π in cells compared to the corresponding levels in the untreated cells ($P<0.05$). In the CDDP+GSH group, the expression of these proteins was significantly enhanced relative to that of the CDDP group ($P<0.05$). It is worth noting that the expression of P-gp was extremely low in the untreated A549 cells, and there was no obvious change in P-gp expression among the four groups ($P>0.05$) similar to the mRNA expression of MDR-1 in the four groups. Because P-gp is encoded by MDR-1, these results suggested that the mRNA and protein levels of P-gp were consistent in A549 cells.

Discussion

CDDP is a commonly used chemotherapy drug and the initial chemotherapy choice for NSCLC. However, drug resistance is a main obstacle in clinical chemotherapy. The exact mechanism of resistance has not yet been fully clarified, although some resistance mechanisms have been reported. One of the most described cellular defense mechanisms involved in resistance is GSH. GSH is crucial for cell survival, and its depletion is a general characteristic not only of apoptosis but also of other types of cell death [21]. In addition, elevated levels of intracellular GSH have been related to resistance [22], particularly to CDDP-induced resistance [9-11]. In this study, by IHC staining, we demonstrated that intracellular GSH level in the GSH group was higher than that of the control group, and cellular GSH level was higher in the CDDP+GSH group than that in the CDDP group. However, in the CDDP group, GSH expression was lower than that in the control group. At the same time, the cell growth inhibition rate and apoptosis rate of A549 cells in response to CDDP was reduced, consistent with previously published reports [18]. In brief, extrinsic GSH could increase cellular GSH levels, and elevated intracellular GSH level was associated with resistance; however, decreased GSH level was related to apoptosis. Meanwhile, the number of cells with classical morphological features of apoptosis by microscopy decreased; in addition, the mRNA expression of pro-apoptotic proteins caspase3, caspase9 and bax increased, while the mRNA level of anti-apoptotic protein bcl-2 decreased. In summary, GSH downregulated the expression of bcl-2 and upregulated the level of bax; moreover, it activated the initiator caspase (caspase9) and effector caspase (caspase3). These results indicated the involvement of intrinsic (mitochondrial) pathway-induced apoptosis in A549 cells in response to CDDP. Therefore, exogenous GSH could induce resistance to CDDP in A549 cells by inactivating the mitochondria-mediated signaling pathway and elevating cellular GSH accumulation.

On the other hand, GSH ester, N-acetyl-L-cysteine (NAC) or S-adenosylmethionine (both precursors of cysteine and precursors of GSH), have been demonstrated to protect against apoptosis [23-25]. Furthermore, treatment with 1 mM NAC, a source of cysteine for GSH synthesis, reduced denbinobin-induced apoptosis in A549 cells by 95.4±2.8% [18] and induced resistance to fluorouracil (5-FU) or mitomycin (MMC) and higher intracellular GSH levels compared to that of the control group in the gastric adenocarcinoma cell line SGC7901 [26]. Moreover, NAC also protected cells from autophagy by preventing autophagosome formation and protein degradation [27, 28]. GSH monomethyl ester, used as a GSH donor, was capable of sensitizing or protecting hepatoma cells against JNK activation and subsequently, aloe-emodin-induced apoptosis [29]. Nevertheless, BSO, an inhibitor of GSH synthesis, increased the sensitivity of SGC7901 cell line [26]. These results indicated that increasing the source of cysteine for GSH synthesis and replenishing GSH level, as well as treatment with exogenous GSH, can cause resistance to anticancer agents.

Data from various studies have shown that drug resistance in cancer cells is generally associated with GST-induced conjugation of diverse antineoplastic agents with GSH, leading to the formation of less toxic GSH-drug complexes (GS-X), which can be readily excreted from cells through P-gp and MRPs [4]. There are several ATP-dependent multidrug resistant drug efflux pumps on cell membranes, known as ATP-binding cassette (ABC), e.g., P-gp encoded by ABCB1 (MDR-1) and MRP1 encoded by ABCC1. P-gp and MRP1 have similar structures and mediate drug resistance in similar manners, but there are several exceptions-taxanes and paclitaxel are substrates for P-gp but have poor affinity for MRP1 [30], whereas CDDP is a substrate for MRP1 but not for P-gp [31]. In the present study, the level of MDR1 was found to be very low at both mRNA and protein levels, consistent with a previous report [32]. Moreover, there was no significant changes in

MDR1 and P-gp expression in the four groups; in other words, the expression of MDR1 and P-gp was independent of CDDP and GSH. These results may be explained by the fact that neither CDDP nor GSH is a substrate of P-gp. P-gp is well known as an efflux pump contributing to multidrug resistance (MDR), but it might not be associated with CDDP-resistance. MRP1 is an important member of the MRP family and is expressed in all tissues [32]. MRP1 can transport anticancer drugs including doxorubicin, etoposide, CDDP and vincristine, all of which require GSH as a substrate [32, 33]. In the presence of GST, GSH and CDDP can form a conjugate called $Pt(GS)_2$, which can be transported via MRP1 [4, 32, 34]. $Pt(GS)_2$ was initially reported by Ishikawa and Ali-Osman to reach a maximal level after 12 h of exposure to 20 μM CDDP, corresponding to 60% of the cellular platinum content in L1210 leukemia cells [35]. Moreover, the $Pt(GS)_2$ complex was found approach in ovarian cancer cells by the [1H,15N] HSQC method [36]. Efflux of $Pt(GS)_2$ ultimately causes reduction in cellular platinum level. Our data demonstrated that in the CDDP+GSH group, the apoptosis rate and intracellular platinum concentration were notably reduced relative to those in the CDDP group. Reduction of cellular platinum uptake in CDDP-resistant cells was observed not only in A549 cells but also in other NSCLC cell lines, such as SKMES-1, MOR and H460 [37]. Furthermore, the expression of MRP1 was enhanced in the CDDP+GSH group compare to that in the CDDP group, and its level was decreased in the CDDP group relative to that in the control group. The trend of MRP1 expression followed an inverse pattern to the sensitivity of A549 cells to CDDP. Several studies have suggested that GSH promotes the refractory response of cancer cells to chemotherapeutics by increasing the expression of MRP1 [38, 39]. These results were consistent with ours.

GST-π is one of the major isoforms of GSTs and plays an important role in cancer development and CDDP-resistance by mediating the formation of GSH-conjugates and subsequent platinum detoxification by acting synergistically with MRP1. GST-π is highly expressed in human cancers [40], and the expression of GST-π has also been found as an independent prognostic indicator of patient outcomes irrespective of chemotherapy [4]. The changes in the level of GST-π was consistent with the trend of MRP1 expression in the four groups but was opposite to the trend of apoptosis in the present study. We speculated that the overexpression of GST-π and MRP1 might contribute to resistance against antineoplastic agents.

The first and rate limiting step of GSH biosynthesis is the formation of γ-glutamylcysteine (γ-GC) catalyzed by γ-GCS (also known as glutamate cysteine ligase, GCL), a heterodimeric holoenzyme composed of a catalytic or heavy subunit (GCLC, 73 kDa) and a modifier or a light subunit (GCLM, 31 kDa), and both GCLC and GCLM activities can affect cellular GSH levels [4, 41]. Therefore, we detected total γ-GCS protein levels by immunohistochemistry but not by Western blotting. γ-GCS activity is regulated by the availability of L-cysteine (Cys), oxidative stress and competitive inhibition via negative feedback by GSH [4, 41, 42]. GSH is synthesized in the cell cytosol and exported across the plasma membrane into the extracellular space, and it is rapidly degraded in circulation by γ-glutamyl transpeptidase (γGT) and dipeptidases (DP) into free amino acids, such as Glu, Cys, and Gly [4, 32]. Then, these amino acids can be pumped into cells and intracellularly resynthesized into GSH. We speculated that the ectopic GSH added to A549 cells would also be broken down into Cys, which would then enhance γ-GCS activity and expression and consequently lead to higher γ-GCS expression and increase the intracellular GSH level in the GSH group than that in the control group. The experimental results confirmed our speculation. We demonstrated that CDDP induced apoptosis in A549 cells. Oxidative stress is a known inducer of cell death, including apoptosis [43]. Accordingly, in the CDDP group, γ-GCS activity and expression, as well as apoptosis, was enhanced by oxidative stress. In the CDDP+DDP group, the γ-GCS expression was significantly increased by the abundance of Cys and oxidative stress. Furthermore, we speculated that cellular GSH levels would be elevated by the increase in γ-GCS expression. However, the GSH system is far more complicated than we can imagine. GSH can be pumped out of cells and is also a substrate for MRP1 [32]. In the GSH group, the elevated cellular GSH level could be explained by the notion that GSH synthesis notably increased and reversed the effect of GSH efflux via negative feedback of GSH. Furthermore, the decrease in GSH level in the CDDP group was correlated with GSH efflux

by CDDP-induced apoptosis. In addition, the results of elevated intracellular GSH level in the CDDP+GSH group compared to that of the CDDP group might be clarified by the speculation that GSH synthesis enhanced and reversed the influence of GSH efflux. In summary, intracellular GSH level decreased with apoptosis and increased with drug resistance.

Numerous studies have displayed the relationship between the level of GSH and bcl-2 expression in cancer cells. Overexpression of bcl-2 in the cell line HeLa, mouse lymphoma cell line LYar and neuroblastoma cell line SK-N-MC increased intracellular GSH levels by altering GSH efflux [44-46]. Rudin et al. transfected MCF-7 cells with bcl-2 and found that bcl-2-overexpression increased cellular GSH level by almost 3-fold and subsequently induced resistance to CDDP [47]. In this study, we also found similar relationship between resistance to CDDP, intracellular GSH level and bcl-2 expression. In summary, apoptotic A549 cells exhibited downregulated bcl-2 expression and decreased GSH level, but resistant A549 cells displayed upregulation of bcl-2 and elevated GSH level.

The GSH system and resistance mechanism are both extremely complex. The correlation between the GSH system and resistance to CDDP is not fully understood. Our recent study has only been performed in vitro, and the human body is equally complicated, and many molecules and cytokines in circulation may influence the effect of GSH. Therefore, the conclusions from the present study should be further validated in vivo. In addition, NSCLC has several subtypes including adenocarcinoma, squamous cell carcinoma, adenosquamous carcinoma and large cell carcinoma. A549 cells belong to a type of adenocarcinoma of the lung. We need to deeply explore the role of GSH in other adenocarcinoma and squamous cell carcinoma cell lines to understand the relationship between extrinsic GSH and resistance.

Conclusions

Our data demonstrated that exogenous GSH used as hepatinica in the clinic could induce resistance of A549 cells to CDDP by inhibiting apoptosis, elevating cellular GSH levels, inactivating the mitochondria-mediated signaling pathway, and promoting the overexpression of GST-π, γ-GCS and MRP1 to increase CDDP efflux. Considering the contribution of GSH in the resistance to CDDP in cells, perhaps we should use other drugs instead of GSH for protecting against liver damage.

Acknowledgements

This study was supported by funds from the National Natural Science Foundation of China (NSFC81560469, NSFC81360327), Guangxi Natural Science Foundation (2015GXNSFCA-139009), Guangxi Medical University Training Program for Distinguished Young Scholars (2017) and Guangxi Health Department Research Project (z2014032).

Disclosure of conflict of interest

None.

Address correspondence to: Zhengwen Cai, Department of Medical Oncology, Second Affiliated Hospital of Guangxi Medical University, No. 166 Daxuedong Road, Nanning 530007, Guangxi Zhuang Autonomous Region, P. R. China. E-mail: 99CCZZWW@sina.com; Gang Chen, Department of Pathology, First Affiliated Hospital of Guangxi Medical University, No. 6 Shuangyong Road, Nanning 530021, Guangxi Zhuang Autonomous Region, P. R. China. E-mail: chen_gang_triones@163.com

References

[1] Spiro SG, Tanner NT, Silvestri GA, Janes SM, Lim E, Vansteenkiste JF and Pirker R. Lung cancer: progress in diagnosis, staging and therapy. Respirology 2010; 15: 44-50.

[2] Chang A. Chemotherapy, chemoresistance and the changing treatment landscape for NSCLC. Lung Cancer 2011; 71: 3-10.

[3] d'Amato TA, Landreneau RJ, McKenna RJ, Santos RS and Parker RJ. Prevalence of in vitro extreme chemotherapy resistance in resected nonsmall-cell lung cancer. Ann Thorac Surg 2006; 81: 440-446; discussion 446-447.

[4] Donald S. Backos, Christopher C. Franklin, Philip Reigan. The role of glutathione in brain tumor drug resistance. Biochem Pharmacol 2012; 83: 1005-1012.

[5] Soini Y, Napankangas U, Jarvinen K, Kaarteenaho-Wiik R, Paakko P, Kinnula VL. Expression of gamma-glutamyl cysteine synthetase in nonsmall cell lung carcinoma. Cancer 2001; 92: 2911-2919.

[6] Tew KD. Glutathione-associated enzymes in anticancer drug resistance. Cancer Res 1994; 54: 4313-4320.

[7] Yang P, Ebbert JO, Sun Z, Weinshilboum RM. Role of the glutathione metabolic pathway in lung cancer treatment and prognosis: a review. J Clin Oncol 2006; 24: 1761-1769.
[8] Gottesman MM. Mechanisms of cancer drug resistance. Annu Rev Med 2002; 53: 615-627.
[9] Mishima K, Baba A, Matsuo M, Itoh Y and Oishi R. Protective effect of cyclic AMP against cisplatin-induced nephrotoxicity. Free Radic Biol Med 2006; 40: 1564-1577.
[10] Sasada T, Nakamura H, Ueda S, Iwata S, Ueno M, Takabayashi A, Yodoi J. Secretion of thioredoxin enhances cellular resistance to cis-diamminedichloroplatinum (II). Antioxid Redox Signal 2000; 2: 695-705.
[11] Jansen BA, Brouwer J and Reedijk J. Glutathione induces cellular resistance against cationic dinuclear platinum anticancer drugs. J Inorg Biochem 2002; 89: 197-202.
[12] Lustberg MB, Edelman MJ. Optimal duration of chemotherapy in advanced non-small cell lung cancer. Curr Treat Options Oncol 2007; 8: 38-46.
[13] Byun SS, Kim SW, Choi H, Lee C, Lee E. Augmentation of cisplatin sensitivity in cisplatin-resistant human bladder cancer cells by modulating glutathione concentrations and glutathione-related enzyme activities. BJU Int 2005; 95: 1086-1090.
[14] Brozovic A, Majhen D, Roje V, Mikac N, Jakopec S, Fritz G, Osmak M, Ambriovic-Ristov A. alpha(v)beta(3) Integrin-mediated drug resistance in human laryngeal carcinoma cells is caused by glutathione-dependent elimination of drug-induced reactive oxidative species. Mol Pharmacol 2005; 74: 298-306.
[15] Dedoussis GV and Andrikopoulos NK. Glutathionedepletion restores t he susceptibility of cisplatin-resistant chronic myelogenous leukemia cell lines to natural killer cell-mediated cell death via necrosis rather than apoptosis. European Journal of Cell Biology 2001; 80: 608-614.
[16] Troyano A, Fernández C, Sancho P, de Blas E, Aller P. Effect of glutathione depletion on antitumor drug toxicity (apoptosis and necrosis) in U-937 human promonocytic cells: the role of intracellular oxidation. J Biol Chem 2001; 276: 47107-47115.
[17] Ikeda K, Miura K, Himeno S, Imura N and Naganuma A. Gluta-thione content is correlated with the sensitivity of lines of PC12 cells to cisplatin without a corresponding change in the accumulation of platinum. Mol Cell Biochem 2001; 219: 51-56.
[18] Kuo CT, Chen BC, Yu CC, Weng CM, Hsu MJ, Chen CC, Chen MC, Teng CM, Pan SL, Bien MY, Shih CH, Lin CH. Apoptosis signal-regulating kinase 1 mediates denbinobin-induced apoptosis in human lung adenocarcinoma cells. J Biomed Sci 2009; 16: 43.
[19] Ovadje P, Chatterjee S, Griffin C, Tran C, Hamm C, Pandey S. Selective induction of apoptosis through activation of caspase-8 in human leukemia cells (Jurkat) by dandelion root extract. J Ethnopharmacol 2011; 133: 86-91.
[20] Rajagopalan V, Hannun YA. Sphingolipid metabolism and signaling as a target for cancer treatment. In cell death signaling in cancer biology and treatment. In: Johnson DE, editor. New York: Springer press; 2013. pp. 205-229.
[21] Ortega AL, Mena S, Estrela JM. Glutathione in cancer cell death. Cancers 2011; 3: 1285-1310.
[22] Kasherman Y, Sturup S and Gibson D. Is glutathione the major cellular target of cisplatin? A study of the interactions of cispatin with cancer cell extracts. J Med Chem 2009; 52: 4319-4328.
[23] Cazanave S, Berson A, Haouzi D, Vadrot N, Fau D, Grodet A, Letteron P, Feldmann G, El-Benna J, Fromenty B, Robin MA, Pessayre D. High hepatic glutathione stores alleviate fas-induced apoptosis in mice. J Hepatol 2007; 46: 858-868.
[24] Franco R, Panayiotidis MI, Cidlowski JA. Glutathione depletion is necessary for apoptosis in lymphoid cells independent of reactive oxygen species formation. J Biol Chem 2007; 282: 30452-30465. 69.
[25] Wang X, Cederbaum AI. S-adenosyl-l-methionine attenuates hepatotoxicity induced by agonistic jo2 fas antibody following cyp2e1 induction in mice. J Pharmacol Exp Ther 2006; 317: 44-52.
[26] Tai DJ, Jin WS, Wu CS, Si HW, Cao XD, Guo AJ, Chang JC. Changes in intracellular redox status influence multidrug resistance in gastric adenocarcinoma cells. Exp Ther Med 2012; 4: 291-296.
[27] Scherz-Shouval R, Shvets E, Fass E, Shorer H, Gil L, Elazar Z. Reactive oxygen species are essential for autophagy and specifically regulate the activity of atg4. EMBO J 2007; 26: 1749-1760.
[28] Yuan H, Perry CN, Huang C, Iwai-Kanai E, Carreira RS, Glembotski CC, Gottlieb RA. Lps-induced autophagy is mediated by oxidative signaling in cardiomyocytes and is associated with cytoprotection. Am J Physiol Heart Circ Physiol 2009; 296: H470-H479.
[29] Lu GD, Shen HM, Chung MC, Ong CN. Critical role of oxidative stress and sustained jnk activation in aloe-emodin-mediated apoptotic cell death in human hepatoma cells. Carcinogenesis 2007; 28: 1937-1945.
[30] Januchowski R, Wojtowicz K, Sujka-Kordowska P, Andrzejewska M, Zabel M. MDR gene ex-

pression analysis of six drug-resistant ovarian cancer cell lines. Biomed Res Int 2013; 2013: 241763.
[31] Stordal B, Hamon M, McEneaney V, Roche S, Gillet JP, O'Leary JJ, Gottesman M, Clynes M. Resistance to paclitaxel in a cisplatin-resistant ovarian cancer cell line is mediated by P-Glycoprotein. PLoS One 2012; 7: e40717.
[32] Zhao M, Lei C, Yang Y, Bu X, Ma H, Gong H, Liu J, Fang X, Hu Z, Fang Q. Abraxane, the nanoparticle formulation of paclitaxel can induce drug resistance by upregulation of P-gp. PLoS One 2015; 10: e0131429.
[33] Ballatori N, Krance SM, Marchan R, Hammond CL. Plasma membrane glutathione transporters and their roles in cell physiology and pathophysiology. Mol Aspects Med 2009; 30: 13-28.
[34] Kuo MT. Redox regulation of multidrug resistance in cancer chemotherapy: molecular mechanisms and therapeutic opportunities. Antioxid Redox Signal 2009; 11: 99-133.
[35] Chen HH, Kuo MT. Role of glutathione in the regulation of cisplatin resistance in cancer chemotherapy. Met Based Drugs 2010; 2010.
[36] Ishikawa T and Ali-Osman F. Glutathione-associated cis-diamminedichloroplatinum(II) metabolism and ATP-dependent efflux from leukemia cells. Molecular characterization of glutathione-platinum complex and its biological significance. J Biol Chem 1993; 268: 20116-20125.
[37] Kasherman Y, Sturup S, Gibson D. Is glutathione the major cellular target of cisplatin? A study of the interactions of cisplatin with cancer cell extracts. J Med Chem 2009; 52: 4319-4328.
[38] Barr MP, Gray SG, Hoffmann AC, Hilger RA, Thomale J, O'Flaherty JD, Fennell DA, Richard D, O'Leary JJ, O'Byrne KJ. Generation and characterisation of cisplatin-resistant non-small cell lung cancer cell lines displaying a stemlike signature. PLoS One 2013; 8: e54193.
[39] Akan I, Akan S, Akca H, Savas B and Ozben T. Multidrug resistance-associated protein 1 (MRP1) mediated vincristine resistance: effects of N-acetylcysteine and buthionine sulfoximine. Cancer Cell Int 2005; 5: 22.
[40] Jin WS, Kong ZL, Shen ZF, Jin YZ, Zhang WK and Chen GF. Regulation of hypoxia inducible factor-1α expression by the alteration of redox status in HepG2 cells. J Exp Clin Cancer Res 2011; 30: 61.
[41] Bredel M, Zentner J. Brain-tumour drug resistance: the bare essentials. Lancet Oncol 2002; 3: 397-406.
[42] Lu SC. Glutatuthione systemsis. Biochim Biophys Acta 2013; 1830: 3143-3153.
[43] Aquilano K, Baldelli S, Ciriolo MR. Glutathione: new roles in redox signaling for an old antioxidant. Front Pharmacol 2014; 5: 12.
[44] Meredith MJ, Cusick CL, Soltaninassab S, Sekhar KS, Lu S, Freeman ML. Expression of Bcl-2 increases intracellular glutathione by inhibiting methionine-dependent GSH efflux. Biochem Biophys Res Commun 1998; 248: 458-463.
[45] Voehringer DW, Meyn RE. Redox aspects of Bcl-2 function. Antioxid Redox Signal 2000; 2: 537-550.
[46] Lee M, Hyun DH, Marshall KA, Ellerby LM, Bredesen DE, Jenner P, Halliwell B. Effect of overexpression of BCL-2 on cellular oxidative damage, nitric oxide production, antioxidant defenses, and the proteasome. Free Radic Biol Med 2001; 31: 1550-1559.
[47] Rudin CM, Yang Z, Schumaker LM, VanderWeele DJ, Newkirk K, Egorin MJ, Zuhowski EG, Cullen KJ. Inhibition of glutathione synthesis reverses Bcl-2-mediated cisplatin resistance. Cancer Res 2003; 63: 312-318.